International Journal of Advances in Engineering and Management (IJAEM)
Volume 5, Issue 2 Feb. 2023, pp: 867-876 www.ijaem.net ISSN: 2395-5252

A Review Study on Thermal analysis of friction stir welding process

Atul Suri[1], D.K. Chaturvedi[2]
[1]Assistant Professor, Dayalbagh Educational Institute, Dayalbagh, Agra, U.P
[2] Professor, Dayalbagh Educational Institute, Dayalbagh, Agra, U.P.

Date of Submission: 18-02-2023 Date of Acceptance: 19-02-2023

ABSTRACT:Friction stir welding is a solid-state joining technique that preserves the properties of the metal being welded. Unlike traditional welding methods, the metal does not melt during the process. Instead, the two metal pieces are mechanically mixed at the joint and then softened, allowing for the application of mechanical pressure to fuse the metal together, similar to joining clay or dough. This technique is commonly used for large pieces of aluminum that cannot be easily heat-treated after welding without compromising their original characteristics.Recent studies have compared the compatibility of different probe shapes and their effect on temperature distribution during the process. The results show that spherical pins generate the highest temperatures in the workpieces, while cylindrical and tapered pins result in lower temperatures. Moreover, increasing the pin angle leads to a higher heat generation in the workpieces.This article reviews relevant literature and presents results from experiments conducted on precipitation-hardening aluminum alloys to shed light on the nature and effects of temperature transients caused by varying thermal boundaries in friction stir welding.

KEYWORDS: Thermal analysis, friction stir welding (FSW), temperature distribution, aluminium alloy, ANSYS.

I. INTRODUCTION

Aluminum alloys have unique properties that make them suitable for various applications. However, traditional joining techniques can lead to cracks due to differences in thermal characteristics. To address this, solid-state welding techniques have been developed, including friction stir welding (FSW). FSW is a solid-state joining method that blends two metal pieces together at the joint without melting the metal, commonly used to preserve the original metal's properties. A cylindrical tool with a profiled, threaded or unthreaded probe is rotated at a constant speed and fed into the joint line, creating frictional heat that softens the materials without melting them. Severe plastic deformation in the solid state facilitates the material's welding. Accurate thermal modeling is crucial to forecasting thermal performance [1] because the amount of heat transferred primarily determines the temperature distribution over the workpiece.

A model is used to calculate stresses and temperatures during friction stir welding (FSW), but it does not take into account the transient variations of variables during the initial tool insertion and final withdrawal periods. The model solves equations for the conservation of mass, momentum, and energy in a steady state, three-dimensional Cartesian coordinate system, considering incompressible single-phase flow. It calculates the three-dimensional heat generation rates, temperature and velocity fields, viscosity, flow stress, strain rate, and torque for various welding conditions and tool and workpiece materials. Although the specifics of the model are already known, this study discusses extending it to calculate bending and maximum shear stresses [2].Friction stir welding (FSW) is widely recognized as an environmentally friendly welding technique due to its smokeless operation. The FSW process utilizes heat generated by the friction between the workpiece and the tool at the weld zone, with additional heat produced by plastic deformation. As a result, FSW produces minimal heat-affected zones and reduces the amount of distortion and residual stresses. The welding conditions, including tool profile and parameters, significantly influence the quality of the joint and must be carefully selected to ensure optimal results [3].The FSW process consists of three simultaneous stages, depending on the relative motion of the tool and workpiece. During the first stage, known as the plunging stage, the rotating tool is forced vertically into the workpiece, generating heat due to friction and plastic deformation of the material. The second stage,

International Journal of Advances in Engineering and Management (IJAEM)
Volume 5, Issue 2 Feb. 2023, pp: 867-876 www.ijaem.net ISSN: 2395-5252

known as the dwell period, involves the rotating tool remaining stationary at the same location without changing its direction of rotation. As a result of the heat being transferred into the workpiece material, the temperature increases and the workpiece material softens. The final stage of the process involves initiating the welding process by moving the tool while keeping the workpiece still or by moving the worktable in opposition to the rotating tool. The tool's advancing side rotates in the same direction as the tool's traversing direction, whereas the tool's retreating side rotates in the opposite direction [4]. Figure 1 shows the principle of FSW operation.

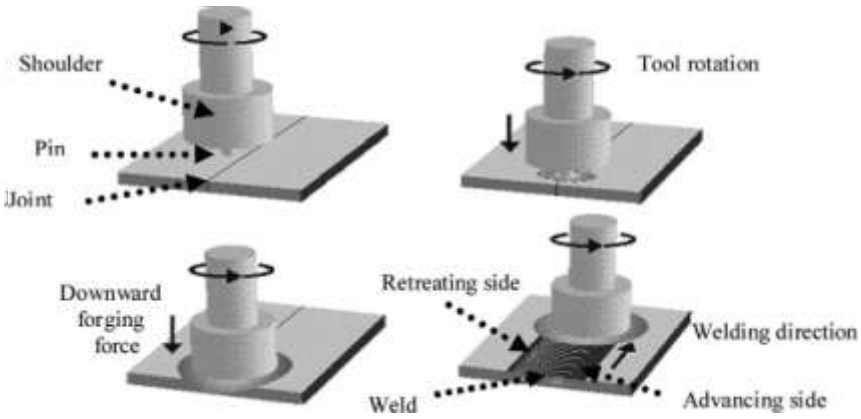

Fig.1. Working Principle of FSW [1]

A review study on the important parameters of thermal analysis is attempted in this paper.

II. THERMAL ANALYSIS

Measuring temperature is crucial in friction stir welding, as it is the most significant load. The temperature sensor records the welding process temperature, which varies depending on the tool profile. When the probe touches the work surface, it generates heat while rotating at a certain depth. While the RPM is constant, the profile and tool parameters change, resulting in different temperatures. For thermal simulations in the ansys software, transient analysis requires temperature parameters over time. We divided the welding process into five steps during actual welding, with each step taking two minutes to complete. We can make assumptions and adjust the time as needed. The table below shows the temperature values for each step relative to temperature. A tool with the highest temperature, for example, would not produce 900°C at its initial level, as the workpiece is around 100mm long, and the total welding time is just ten minutes [3].In summary, friction stir welding's most important load is temperature, which is measured to create a thermal simulation. The welding process is divided into five two-minute steps, and temperature parameters are given for each step-in relation to time, as shown in the table. The temperature varies depending on the tool profile, and RPM remains constant, but the profile and tool parameters change.

Table 1: Temperature of the tool at each step.

Tool No.	Initial Temp ^{o}C	Step 1 (2 min)^{O}C	Step 2 (2 min)^{O}C	Step 3 (2 min)^{O}C	Step 4 (2 min)^{O}C	Step 5 (2 min)^{O}C
1	30	125	385	524	746	917
2	30	118	367	565	759	989
3	30	127	357	551	784	920

International Journal of Advances in Engineering and Management (IJAEM)
Volume 5, Issue 2 Feb. 2023, pp: 867-876 www.ijaem.net ISSN: 2395-5252

III. NATURE OF TEMPERATURE TRANSIENTS IN THE HEAT AFFECTED ZONE

In friction stir welding, it is essential to measure temperatures at various points on a tool to understand the temperature in the stir zone accurately. However, it is equally important to consider far-field temperatures and their impact on the metallurgical changes that occur in the heat-affected zone (HAZ) for precipitation-hardening alloys. Figure 2 provides a visual representation of the typical weld thermal cycle for welds made at 3.4 mm/s in AA7050 under IA, UW, and SA conditions. The information was gathered from temperature sensors placed at HAZ minimum hardness locations identified by prior identical weld runs. For all cases, the peak temperature in the HAZ minimum hardness region is very close to 350C. This is consistent with the temperatures associated with the maximum averaging kinetics of alloys in the AA7XXX series, which results in the HAZ's minimum hardness.Figure 3 shows the cooling rates calculated from similar thermal cycles as those in Figure 2, but for different welding speeds. The cooling rates were calculated between 250 and 320 degrees Celsius. Although the difference between the UW and SA cases is slight, it is clear that the cooling rates in the HAZ in the UW and SA cases are higher than for the IA case. This suggests that for the conditions investigated, sub ambient conditions do not provide a faster cooling rate than what is already possible with water at room temperature. This finding may be relevant to welding under challenging environmental conditions such as those found in the Arctic. Rosenthal's moving-heat-source equations, which show that temporal length correlates inversely with heat source speed, explain this.Figure 4 presents cooling rate information obtained from temperatures measured at HAZ locations corresponding to friction stir welds made in 4.2-mm-thick AA6056 using various backing plates (BPs) with greatly varied thermal diffusivity. The graph shows that the thermal diffusivity of the BP material and the rate of cooling have a logarithmically linear relationship. Using similar equipment to weld relatively thick (25.4 mm) AA6061 plate revealed significantly lower cooling rates (nearly 7C/s). Thinner plates (AA7050 and AA6056) exhibit much higher cooling rates (40C/s) for the same welding speed and thermal boundary condition, [5] as mentioned earlier.

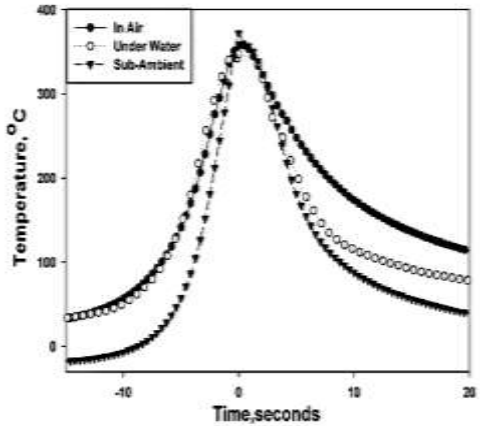

Fig. 2. Temperature history at HAZ minimum hardness location for three different ambient conditions for FSW of 6.35 mm AA7050

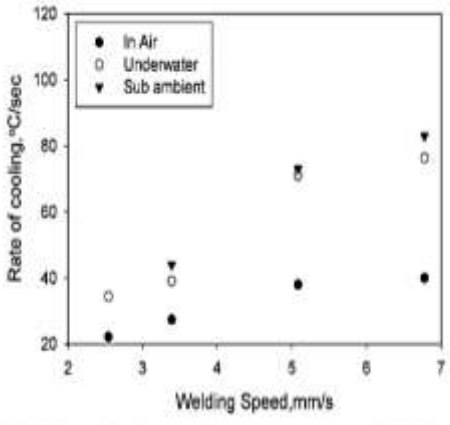

Fig. 3. Rate of cooling over the temperature range of 250oC to 320oC obtained from temperature history measured in the HAZ in FSWs made in 6.35-mm-thick AA7050. [6]

International Journal of Advances in Engineering and Management (IJAEM)
Volume 5, Issue 2 Feb. 2023, pp: 867-876 www.ijaem.net ISSN: 2395-5252

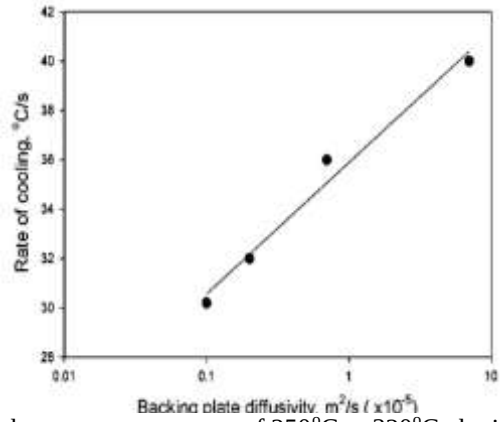

Fig. 4. Rate of cooling over the temperature range of 250°C to 320°C obtained from temperature history measured in the HAZ in FSW of 4.2-mm-thick AA6056 welds[6].

IV. EFFECTS OF THERMAL BOUNDARY CONDITIONS OF WELD PROPERTIES

The figure 5 depict the midplane hardness distributions and post-welding heat treatment (PWHT) of welds made in 6.35 mm thick AA7050-T7 under three different ambient conditions: IA, UW, and SA. The base metal regions exhibit T7 (slightly overaged) hardness, while the nugget region has hardness comparable to a T6 temper. The hardness distribution's shape suggests that the nugget region was almost solution-heated before post-weld aging. The HAZ shows significant averaging that results in a minimum in hardness. The hardness minima in the SA and UW welds are not as deep as in the IA weld, and the HAZ is narrower overall. The higher cooling rates observed in the UW and SA cases, as shown in Figs. 2 and 3, explain both observations. A higher cooling rate produces a stronger and narrower HAZ, shortening the exposure time in the temperature range (350C) of the maximum coarsening kinetics of precipitate phases.Figure 6 shows the HAZ minimum hardness from a series of welds made with various welding and rotational speeds with different boundary conditions. The graph reveals [6] that welding speed has a significant impact on the minimum hardness in the HAZ. Welding at low temperatures or with active cooling raises the HAZ minimum hardness. The minimum hardness values for UW and SA welds are consistently higher than those for IA welds made at the same welding speed due to faster cooling rates at the HAZ. At lower welding speeds, the difference between the minimum hardness values of UW and IA welds is greater, indicating a greater influence of the thermal boundary conditions[7]. The graph also demonstrates that the relationship between the minimum hardness increase and welding speed is nonlinear. At low welding speeds, the increase is rapid, but as welding speed is raised, the increase becomes slower. Above a welding speed of 5.1 mm/s, almost no increase in minimum hardness is seen for UW welds. This finding suggests that increasing the welding speed past a certain point only slightly improves the weld properties.Figure 7 presents tensile-test data from welds made in 25.4-mm-thick AA6061 with different backing plate (BP) types (conventional steelonly, steel/aluminum composite,titanium/aluminum composite, and aluminum only). The figures illustrate that the BP diffusivity significantly affects the joints' tensile strength and ductility. Using aluminum as a BP instead of the more common steel results in a 25% increase in strength, and the elongation of welded joints significantly increases from 3% to 12%. This is because of the reduced strain localization during transverse loading of the nugget's minimum hardness and HAZ minimum hardness of the weld [8] joints. Using a low-diffusivity BP beneath the composite BP, which enabled homogeneous through-thickness nugget temperature, produced higher strength and elongation values in the stir zone compared to the monolithic steel BP. This finding is consistent with the higher cooling rates observed in the HAZ when using a thermodiffusivity BP (see Fig. 4).

International Journal of Advances in Engineering and Management (IJAEM)
Volume 5, Issue 2 Feb. 2023, pp: 867-876 www.ijaem.net ISSN: 2395-5252

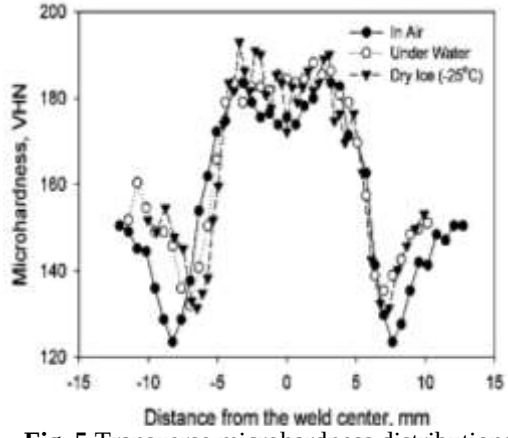

Fig. 5. Transverse microhardness distributions across the midplane of friction-stir welded AA7050-T7 PWHT to T6 with three different ambient conditions: in air, underwater, and under a mixture of dry ice and ethylene glycol.

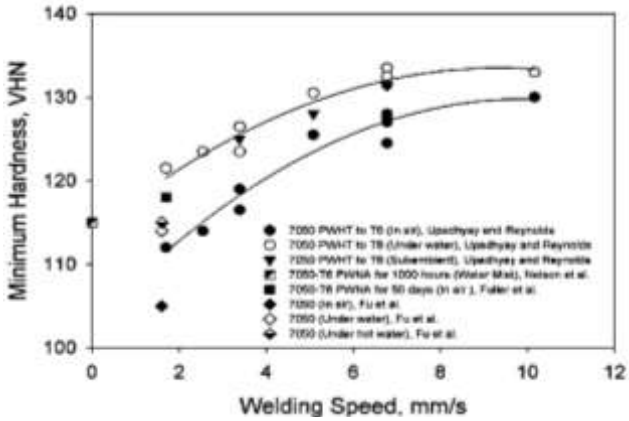

Fig. 6. Average HAZ minimum hardness plotted against the welding speed obtained from different sets of FSW in 7xxx series aluminum alloys using various thermal boundary conditions.

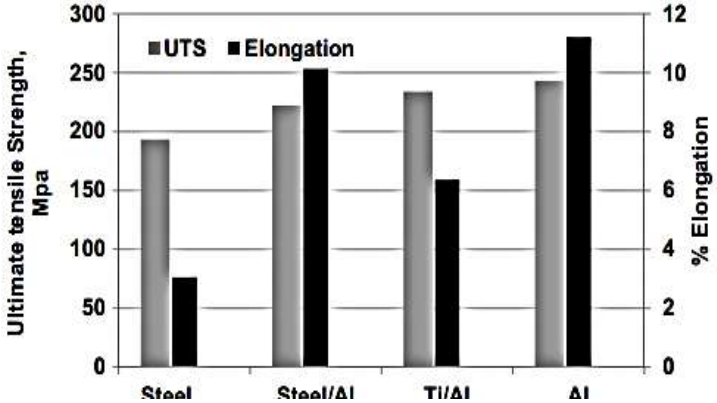

Fig. 7. Transverse tensile strength and percentage elongation of welds made in 25.4-mm-thick AA6061-T6 using different types of BPs.

V. THE EFFECT OF PIN SHAPE

A study was conducted to investigate the effect of probe shape on temperature distribution during friction stir welding. Three different probe shapes were tested: semi-spherical (SPH), tapered cylindrical (TC), and straight cylindrical (SC), as shown in Figure 8. The results (Figure 9) showed that the SPH and SC probes produced the highest and lowest temperatures, respectively, at a specific point along the weld line, except during the pin contact time. The TC probe produced temperatures between those of the SPH and SC probes. Thomas and Nicolas established a correlation between pin profiles and eccentricity and introduced a ratio to describe the interaction between static and dynamic volumes. The ratio was found to be 1 for SC probes, 2.3 for TC probes, and 3.1 for SPH probes, which was consistent with the simulation results. The ratio indicates that as it increases, more material deforms plastically, resulting in greater heat generation and higher temperatures. [9]

VI. THE EFFECT OF PIN ANGLE

Friction stir welding requires careful consideration of the spindle or tool's tilt angle with respect to the workpiece surface. A proper tilt in the trailing direction ensures that the tool's shoulder holds and stirs the material, moving it effectively from the front to the back of the pin. The insertion depth of the pin into the workpiece, or target depth, is also crucial for producing strong welds with smooth tool shoulders. The impact of four different pin angles (0, 5, 10, and 15 degrees) on temperature distribution was investigated, and the resulting distributions are shown in Fig. 10.

International Journal of Advances in Engineering and Management (IJAEM)
Volume 5, Issue 2 Feb. 2023, pp: 867-876 www.ijaem.net ISSN: 2395-5252

The findings suggest that an increase in pin angle leads to a rise in temperature, potentially due to an increase in the contact area between the pin and workpiece, which generates more friction and heat. Additionally, the temperature increase could be attributed to an increase in redundant work resulting from the larger pin angle. Previous research has also noted the production of heat due to friction and redundant work during metalworking processes. [10,11].

VII. HETA GENERATION FROM PIN TOOL NIB

The pin tool nib was not included in the current simulation to prevent mesh locking, which can be caused by incompressible plastic deformation. However, it's worth noting that the pin nib and the tool shoulder produce different amounts of heat during the welding process. According to Schmidt's study, there is a 16% difference in heat production between the two. To account for the heat flow from the pin tool nib, the heat generated by friction with the workpiece and plastic deformation in the model was adjusted by multiplying it by a factor of 1.16[12].

VIII. EFFECT OF PLUNGE FORCE ON WELDING

To examine the effect of plunge force, a parametric analysis was conducted, considering three different plunge forces: 12.455, 15.568, and 21.351 kN, while keeping rotational speed and travel speed constant. After 27 seconds of simulation, the frictional dissipation energy was calculated for all three plunge force cases, as shown in Figure 11. The results indicate that the energy increases as the plunge force increases. Specifically, when the plunge force was raised from 12.455 to 21.351 kN, the overall frictional dissipation energy increased by 22.96%. Similarly, when the plunge force was raised from 15.568 to 21.351 kN, the frictional dissipation energy increased by 21.48%. This is because a higher plunge force causes more material to penetrate and rotate, leading to greater energy [13] generation. Table 2 summarizes the effect of plunge force on frictional energy [14].

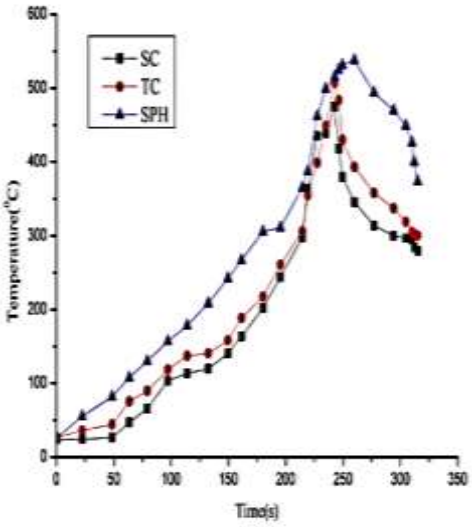

Fig. 9. Temperature variations of a definite point of weld line when different pins are used (SC, TC and SPH stand respectively for straight cylindrical, tapered cylindrical and spherical pins)[10].

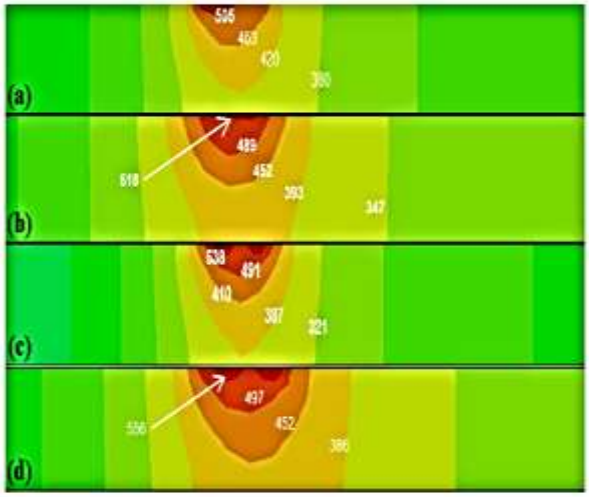

Fig. 10. Temperature distribution around the weld line for different values of pin angle; (a) 0º; (b) 5º; (c) 10º; (d) 15º

International Journal of Advances in Engineering and Management (IJAEM)
Volume 5, Issue 2 Feb. 2023, pp: 867-876 www.ijaem.net ISSN: 2395-5252

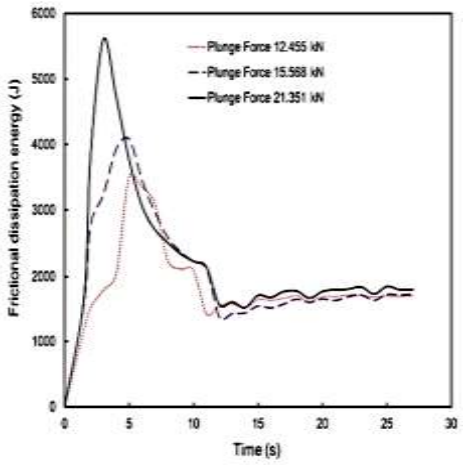

Fig. 11 Frictional dissipation energy variation with plunge force (ω = 350 rpm, v = 1.27 mm/s)

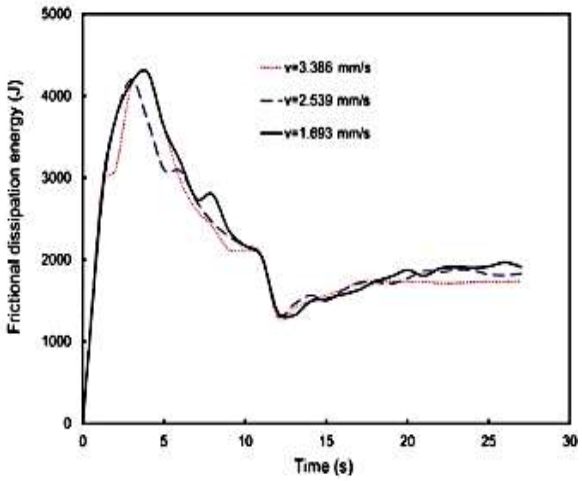

Fig. 12 Frictional dissipation energy variation with welding speed (Fz = 26.68 kN,**ω**= 300 rpm)

Table 2: Summary of friction dissipation energies for various plunge force

Rotational speed, ω (rpm)	Traverse speed, V (mm/s)	Plunge force, F_Z, (kN)	Frictional energy (J)		Frictional energy percentage increase
350	1.27	12.455	1.04×10^6		22.96%
350	1.27	15.568	1.06×10^6		21.48%
350	1.27	21.351	1.35×10^6		Base1

IX. EFFECT OF WELDING SPEED

To examine the impact of tool travel speed on frictional dissipation energies, three different weld speeds were taken into account: 3.386, 2.539, and 1.693 mm/s, with a constant plunge and rotational speed of ω= 300 rpm. A force of Fz = 26.68 kN was used in these analyses. The results showed that as the welding speed decreased, the frictional dissipation energy increased. For instance, when the travel speed was reduced from 3.386 to 1.693 mm/s, the overall frictional dissipation energy increased by about 5.40% [15]. Similarly, when the travel speed was reduced from 2.539 to 1.693 mm/s, the overall frictional dissipation energy increased by about 4.50%. This suggests that the tool's slower travel speed provides more time for the material to rotate, leading to a faster rate of local heat generation. Figure 12 illustrates these results.Furthermore, decreasing the travel speed from 2.539 to 1.693 mm/s resulted in an approximately 4.50% increase in overall frictional dissipation energy. This is because the slower travel speed of the tool allows for a longer rotation time for the material, which in turn increases the local heat generation rate [14].

X. EFFECT OF WELDING SPEED

To investigate the effect of the rotational speed of welding tools, the analysis considered rotational speeds of 200, 300, 400, and 450 rpm, while the travel speed was kept constant at V = 2.539 mm/s. A constant plunge force of Fz = 26.68 kN was used. Figure 13 shows that higher frictional dissipation energy was produced at faster rotational speeds. When the rotational speed increased from 200 to 450 rpm, the overall frictional dissipation energy increased by around 80.06%. Additionally, the total frictional energy increased by approximately 32.25% when the rotational speed was raised from 300 to 450 rpm. This is due to the rapid rotation of the materials, which leads to an increase in their relative velocities and the generation of more energy [16]. The impact of rotational speed on frictional dissipation energy is summarized in Table 3 [14].

International Journal of Advances in Engineering and Management (IJAEM)
Volume 5, Issue 2 Feb. 2023, pp: 867-876 www.ijaem.net ISSN: 2395-5252

Table 3: Summary of friction dissipation energies for various rotational speeds

Rotational speed, **ω**,(rpm)	Traverse speed, V (mm/s)	Plunge force, F_Z, (kN)	Total frictional energy(J)	Frictionalenergy percentageincrease
200	2.539	26.68	3.09×10^5	80.06
300	2.539	26.68	1.05×10^6	32.25
450	2.539	26.68	1.55×10^6	Base2

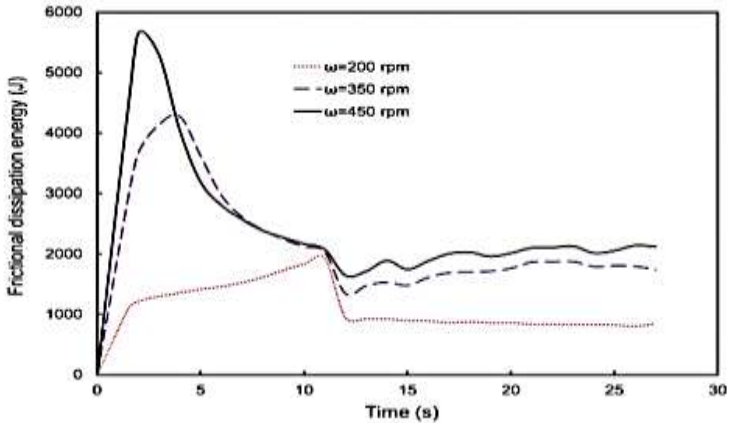

Fig. 13 Frictional dissipation energy variation with rotational speed(v = 1.27 mm/s, Fz = 26.68 kN)

XI. CONCLUSION

The impact of various weld parameter viz plunge force, rotational speed, and travel speed—was examined using a parametric study. The study's findings showed that

(a) The energy generated by friction dissipation increased with increasing plunge force. When the plunge force is increased from 12.455 to 21.351 kN, the total frictional dissipation energy increases by 23 and 21%.

(b) The total amount of frictional dissipation energy increases with rotational speed.

Total frictional energy increases to 80.06% and 32.25%, respectively, when rotational speed is increased from 200 to 450 rpm.

(c) Slower travel speeds result in more overall frictional and plastic energy loss. Total frictional changes from 5.40% to 4.50%, respectively, when travel speed changes from 3.386 to 1.693 mm/s.

- Among the three major FSW process parameters, the effect of rotational speed on generating frictional energy is found to be the most important parameter.
- During the FSW process, straight cylindrical pins produce less heat and correspondingly lower temperatures than tapered cylindrical pins, and both are lower than those attained with semi-spherical pins.
- As pin angle increases, because of frictional heat generated during FSW, the temperature of workpieces increases.
- Numerousprecipitation-hardeningaluminium alloys have undergone FSW using a variety of thermal management techniques in a range of thicknesses. Reduced nugget temperature, increased torque, and increased cooling rate in the HAZ were all produced as a result of active cooling, with all other variables remaining constant. Higher HAZ minimum hardness and higher tensile strength of tested transverse weld cross-sections were the results of the HAZ's increased cooling rate as a result of improved surface convection. Hardness measurements and temperature measurements at the HAZ showed that welding above a certain welding speed only slightly lengthens the time at temperature. This shows that property enhancement returns are limited above a certain welding speed. Thermal-cycle and hardness measurements conducted under the investigated circumstances reveal that precooling the workpiece to 25C results in a property benefit comparable to that obtained from welding in water at ambient temperature, albeit with significantly more effort. The peak temperature reached at the weld nugget and the rate of cooling in the HAZ are both significantly influenced by the thermal diffusivity of the BP material, which causes a significant variation in the weld properties. Simply by switching the BP material, a wide range of forge force may be used to produce

welds without defects. While a high-thermal-diffusivity BP can improve cooling, using a low-thermal-diffusivity BP enables homogeneous weld temperature in relatively thick sections. A high-thermal-diffusivity BP can improve cooling rates in the HAZ, resulting in improved HAZ minimum hardness, whereas a low-thermal-diffusivity BP allows for homogeneous weld temperature in relatively thick sections.

- This study's main goal is to gain a better understanding of temperature distribution and material flow at each stage of the FSW process. The temperature distribution that was discovered to be in good conformity between experimental observations and numerical simulations. The maximum temperature for FSW has been confirmed to be between 80% and 90% of its melting point temperature, which is below the process's theoretical working temperature range. It has been noted that longer periods of residence may lead to higher temperature generation. On both sides of the welded plate, the temperature distribution is found to be asymmetrical. The tool's rotational speed should be increased while welding speed should be decreased to increase heat generation and the resulting high temperature.

REFERENCES

[1]. C. Chalurkar and D. K. Shukla, "Temperature Analysis of Friction Stir Welding (AA6061-T6) with Coupled Eulerian-Lagrangian Approach.," IOP Conf. Ser. Mater. Sci. Eng., vol. 1248, no. 1, p. 012035, 2022, doi: 10.1088/1757-899x/1248/1/012035.

[2]. D. M. V. M. I. Ajit Kumar, "Thermal Analysis of Friction Stir Welding," Int. J. Eng. Res. Technol., vol. 4, no. 2, pp. 0–4, 2015, [Online]. Available: www.ijert.org

[3]. P. Jayaseelan, S. Rajesh Ruban, M. Suresh, N. S. Gowtham, and P. Saravanan, "Thermal analysis of pentagonal profiled friction stir welding tool using Ansys," IOP Conf. Ser. Mater. Sci. Eng., vol. 993, no. 1, 2020, doi: 10.1088/1757-899X/993/1/012144.

[4]. P. Dong, H. Li, D. Sun, W. Gong, and J. Liu, "Effects of welding speed on the microstructure and hardness in friction stir welding joints of 6005A-T6 aluminum alloy," Mater. Des., vol. 45, pp. 524–531, 2013, doi: 10.1016/j.matdes.2012.09.040.

[5]. E. G. Cole, A. Fehrenbacher, N. A. Duffie, M. R. Zinn, F. E. Pfefferkorn, and N. J. Ferrier, "Weld temperature effects during friction stir welding of dissimilar aluminum alloys 6061-t6 and 7075-t6," Int. J. Adv. Manuf. Technol., vol. 71, no. 1–4, pp. 643–652, 2014, doi: 10.1007/s00170-013-5485-9.

[6]. P. Upadhyay and A. P. Reynolds, "Tphermal management in friction-stir welding of preciitation-hardened aluminum alloys," Jom, vol. 67, no. 5, pp. 1022–1031, 2015, doi: 10.1007/s11837-015-1381-0.

[7]. B. C. Liechty and B. W. Webb, "Modeling the frictional boundary condition in friction stir welding," Int. J. Mach. Tools Manuf., vol. 48, no. 12–13, pp. 1474–1485, 2008, doi: 10.1016/j.ijmachtools.2008.04.005.

[8]. V. Soundararajan, S. Zekovic, and R. Kovacevic, "Thermo-mechanical model with adaptive boundary conditions for friction stir welding of Al 6061," Int. J. Mach. Tools Manuf., vol. 45, no. 14, pp. 1577–1587, 2005, doi: 10.1016/j.ijmachtools.2005.02.008.

[9]. I. Sukmana, "The Effect of Pin Shape on the Friction Stir Welding Quality of Aluminum AA1100 Series," J. Eng. Sci. Res., vol. 4, no. 1, pp. 45–49, 2022, doi: 10.23960/jesr.v4i1.109.

[10]. M. Abbasi, B. Bagheri, and R. Keivani, "Thermal analysis of friction stir welding process and investigation into affective parameters using simulation," J. Mech. Sci. Technol., vol. 29, no. 2, pp. 861–866, Feb. 2015, doi: 10.1007/s12206-015-0149-3.

[11]. R. Keivani, B. Bagheri, F. Sharifi, M. Ketabchi, and M. Abbasi, "Effects of pin angle and preheating on temperature distribution during friction stir welding operation," Trans. Nonferrous Met. Soc. China (English Ed., vol. 23, no. 9, pp. 2708–2713, 2013, doi: 10.1016/S1003-6326(13)62788-0.

[12]. W. H. KHALAFE, "the Effect of Friction Stir Welding Parameters on the Weldability of Aluminum Alloys Aa6061 and Aa5083," Αγαη, no. November, p. 102, 2019, doi: 10.20944/preprints202211.0019.v1.

[13]. D. Sethi, U. Acharya, S. Shekhar, and B. S. Roy, "Applicability of unique scarf joint configuration in friction stir welding

of AA6061-T6: Analysis of torque, force, microstructure and mechanical properties," Def. Technol., vol. 18, no. 4, pp. 567–582, 2022, doi: 10.1016/j.dt.2021.03.010.

[14]. S. B. Aziz, M. W. Dewan, D. J. Huggett, M. A. Wahab, A. M. Okeil, and T. W. Liao, "Impact of Friction Stir Welding (FSW) process parameters on thermal modeling and heat generation of aluminum alloy joints," Acta Metall. Sin. (English Lett., vol. 29, no. 9, pp. 869–883, 2016, doi: 10.1007/s40195-016-0466-2.

[15]. T. Sakthivel, G. S. Sengar, and J. Mukhopadhyay, "Effect of welding speed on microstructure and mechanical properties of friction-stir-welded aluminum," Int. J. Adv. Manuf. Technol., vol. 43, no. 5–6, pp. 468–473, 2009, doi: 10.1007/s00170-008-1727-7.

[16]. J. Yan, M. A. Sutton, and A. P. Reynolds, "Process-structure-property relationships for nugget and heat affected zone regions of AA2524-T351 friction stir welds," Sci. Technol. Weld. Join., vol. 10, no. 6, pp. 725–736, 2005, doi: 10.1179/174329305X68778.